Atherosclerosis 285 (2019) 120–127

Contents lists available at ScienceDirect

Atherosclerosis

journal homepage: www.elsevier.com/locate/atherosclerosis

Automated detection of superficial macrophages in atherosclerotic plaques using autofluorescence lifetime imaging

Jose J. Rico-Jimenez[a], Michael J. Serafino[a], Sebina Shrestha[a], Xi Chen[a], Wihan Kim[a], Jessie Adame[b], L. Maximillan Buja[c], Deborah Vela[c], Brian E. Applegate[a], Javier A. Jo[a,d,*]

[a] Department of Biomedical Engineering, Texas A& M University, College Station, TX, USA
[b] Autopsy and Pathology Services, Houston, TX, USA
[c] Texas Heart Institute, Houston, TX, USA
[d] School of Electrical and Computer Engineering, University of Oklahoma, Norman, OK, USA

HIGHLIGHTS

- Plaque autofluorescence lifetime is correlated with superficial macrophage accumulation in coronary atherosclerotic plaques.
- Plaque autofluorescence lifetime can discriminate superficial macrophage accumulation in coronary atherosclerotic plaques.
- Intravascular fluorescence lifetime imaging has the potential for in vivo macrophage imaging of coronary atherosclerosis.

ARTICLE INFO

Keywords:
Plaque characterization
Fluorescence lifetime imaging
Macrophage foam cells
Medical and biological imaging
Image analysis
Classification

ABSTRACT

Background and aims: Macrophages play an important role in the development and destabilization of advanced atherosclerotic plaques. Hence, the clinical imaging of macrophage content in advanced plaques could potentially aid in identifying patients most at risk of future clinical events. The lifetime of the autofluorescence emission from atherosclerotic plaques has been correlated with lipids and macrophage accumulation in *ex vivo* human coronary arteries, suggesting the potential of intravascular endogenous fluorescence or autofluorescence lifetime imaging (FLIM) for macrophage imaging. The aim of this study was to quantify the accuracy of the coronary intima autofluorescence lifetime to detect superficial macrophage accumulation in atherosclerotic plaques.

Methods: Endogenous FLIM imaging was performed on 80 fresh postmortem coronary segments from 23 subjects. The plaque autofluorescence lifetime at an emission spectral band of 494 ± 20.5 nm was used as a discriminatory feature to detect superficial macrophage accumulation in atherosclerotic plaques. Detection of superficial macrophage accumulation in the imaged coronary segments based on immunohistochemistry (CD68 staining) evaluation was taken as the gold standard. Receiver Operating Characteristic (ROC) curve analysis was applied to select an autofluorescence lifetime threshold value to detect superficial macrophages accumulation.

Results: A threshold of 6 ns in the plaque autofluorescence lifetime at the emission spectral band of 494 ± 20.5 nm was applied to detect plaque superficial macrophages accumulation, resulting in ~91.5% accuracy.

Conclusions: This study demonstrates the capability of endogenous FLIM imaging to accurately identify superficial macrophages accumulation in human atherosclerotic plaques, a key biomarker of atherosclerotic plaque vulnerability.

1. Introduction

Atherosclerosis is the leading cause of morbidity and mortality in the United States [1]. It is characterized as a systemic, progressive disease in which the arterial wall thickens through a process of inflammation [2], oxidative stress, and dyslipidemia [3]. This process leads to plaque formation and flow restriction in the vessel lumen. These arterial plaques may also rupture leading to sudden thrombosis and occlusion of the vessel, and ultimately to myocardial infarction, stroke, or limb injury [4].

* Corresponding author. 101 David L. Boren Blvd., Norman, OK, 73019, USA.
E-mail address: javierjo@ou.edu (J.A. Jo).

https://doi.org/10.1016/j.atherosclerosis.2019.04.223
Received 9 August 2018; Received in revised form 8 April 2019; Accepted 16 April 2019
Available online 19 April 2019

The most common underlying plaque morphology leading to myocardial infarction comprises a thin ruptured fibrous cap with heavy macrophage infiltration and few smooth muscle cells, large necrotic core and overlying intraluminal thrombosis [5]. In advanced lesions, macrophages have an impaired ability to efferocytose apoptotic cells [6,7], and macrophage apoptosis and necrosis is increased [8,9]; altogether, these factors contribute to plaque necrosis and increased inflammation. Macrophages in advanced lesions also secrete matrix metalloproteinases, which can contribute to fibrous cap thinning and plaque rupture [10]. Macrophages thus play an important role in the development of advanced lesions, in particular necrotic core formation, which destabilizes the lesion and thereby promotes acute clinical cardiovascular events [11]. Hence, the clinical imaging of macrophage content in advanced plaques could potentially aid in identifying patients most at risk of future clinical events [12].

The improved understanding of the role of macrophages in advance lesions is also enabling exploring alternative therapeutic strategies targeting proatherogenic mechanisms in macrophages, which can be additive or synergistic with current lipid-lowering therapy to further reduce the risk of cardiovascular events. For instance, development of treatment strategies to prevent plaque necrosis or improve efferocytosis in advanced lesions might lead to the prevention of plaque rupture [13–15]. A major challenge in these translational efforts, however, is the ability to assess efficacy of potential therapeutic strategies in humans before committing to expensive and long-term end point trials. As such, parallel developments in macrophage-based imaging will be essential as mechanistic and preclinical studies progress [11,12].

A number of noninvasive imaging modalities are being evaluated for imaging macrophages in atherosclerotic plaques. ^{18}F-fluorodeoxyglucose (^{18}F-FDG) is a radio-labeled glucose analogue used commonly in PET imaging for a variety of diagnostic purposes. In atherosclerosis, vascular ^{18}F-FDG uptake reflects increased activity of macrophages [16,17]; however, ^{18}F-FDG is not a specific marker of plaque inflammation [18], and high myocardial muscle cell uptake often prevents interpretation of coronary signals [19]. Ultrasmall superparamagnetic iron oxide (USPIO) particles generate MRI signal drop when internalized by macrophages [20–22], which has been detected in patients with symptomatic carotid plaques and correlates to macrophage-rich plaque areas [23,24]. However, MRI imaging of macrophages has been limited to carotid arteries and has not been translated yet to the smaller and constantly moving coronary arteries, in part, because the relatively low contrast provided by USPIO particles. Although noninvasive imaging modalities have the potential for imaging plaque macrophages, they still present several hurdles, particularly when focused on small and constantly moving coronary arteries, including the need of radiation exposure and exogenous contrast agents, limited spatial resolution, and susceptibility to motion artifacts [12].

A number of intravascular imaging modalities have also been explored for imaging plaque macrophages. In an *ex vivo* study, intravascular optical coherence tomography (OCT) was used to quantify macrophages within the fibrous cap, seen as bright spots with higher signal intensity than surrounding structures [25]. Further work, however, has revealed that only 23% of bright-spot positive regions on OCT specifically represent macrophages alone [26]. Intravascular near-infrared fluorescence (NIRF) imaging of indocyanine green (ICG), in combination with OCT, was shown to be correlated with the accumulation of lipids and macrophages within atherosclerotic plaques in a rabbit model [27]. The lifetime of the endogenous fluorescence emission from atherosclerotic plaques has also been associated to lipids and macrophage accumulation in *ex vivo* human coronary arteries, suggesting the potential of intravascular endogenous fluorescence lifetime imaging (FLIM) for macrophage imaging [28,29]. Due to its superior spatial resolution, intravascular imaging modalities have the potential for imaging macrophages in coronary arteries; however, their sensitivity and specificity for clinically detecting macrophages still need to be confirmed.

In the current study, endogenous FLIM imaging of *ex vivo* coronary segments were performed in order to quantify the accuracy of the coronary intima autofluorescence lifetime to detect intimal superficial macrophage infiltration. Immunohistochemistry evaluation of the imaged tissue was used as the gold standard for validation. The results of this study indicate that the coronary intima autofluorescence lifetime measured at an emission band of ~475–515 nm is linearly correlated with superficial macrophage density, and enables accurate identification of regions of atherosclerotic plaques with superficial macrophage infiltration.

2. Materials and methods

2.1. FLIM instrumentation, imaging and processing

The approach presented here makes use of FLIM images acquired from the lumen side of fresh postmortem human coronary segments. These artery segments were obtained from 23 autopsy cases within 48 h of the time of death, according to a protocol approved by the Texas A&M University Institutional Review Board (IRB2015-3017M). The multispectral FLIM system used in this work was previously described in Ref. [30]; however, only the signal collected from the 494 ± 20.5 nm spectral channel was used for the identification of macrophages. The excitation source for the FLIM system is a frequency tripled Q-switched Nd:YAG pulsed laser (excitation wavelength: 355 nm; repetition rate: 12.5 kHz; pulse width: 2 ns; pulse energy at the sample: 1 μJ). The fluorescence intensity at the aforementioned spectral emission was detected with a micro-channel-plate photomultiplier (transient time spread: 25 ps) and digitized at a sampling frequency of 4 GHz. The lateral resolution was 120 μm, and the field of view was 16 × 16 mm^2. FLIM images were acquired at a pixel rate of 12.5 kHz.

The fluorescence lifetime maps were computed from the time-resolved fluorescence signal measured at each pixel using a standard instrument response deconvolution method [31]. The fluorescence decay response was assumed to follow a bi-exponential model (Eq. (1)), and an iterative nonlinear least square model parameter estimation was applied. The average fluorescence lifetime for each pixel (Eq. (2)) was estimated from the deconvolved fluorescence decay [32].

Bi-exponential model:

$$\boldsymbol{h}(\boldsymbol{x}, \boldsymbol{y}, \boldsymbol{t}) = \sum_{\boldsymbol{i}=1}^{2} \boldsymbol{\alpha_i}(\boldsymbol{x}, \boldsymbol{y})\, \boldsymbol{e}^{-\boldsymbol{t}/\boldsymbol{\tau_i}(\boldsymbol{x},\boldsymbol{y})} \tag{1}$$

Average lifetime:

$$\boldsymbol{\tau_{avg}}(\boldsymbol{x}, \boldsymbol{y}) = \frac{\sum \boldsymbol{t}\, \boldsymbol{h}(\boldsymbol{x}, \boldsymbol{y}, \boldsymbol{t})}{\sum \boldsymbol{h}(\boldsymbol{x}, \boldsymbol{y}, \boldsymbol{t})} \tag{2}$$

2.2. FLIM database

The database consists of FLIM images of 80 artery segments (from 23 subjects) with their corresponding histological sections stained with CD68 for labeling macrophages (246 histological sections in total). The artery segments were obtained from subjects that not necessarily died from atherosclerosis. The histology sections were cut from specific points previously inked on the right side of the artery lumen, in order to match the histology and the FLIM images (Fig. 1A). The top edge of the artery was also inked and a small notch was made at the bottom to help find the correct orientation. Each dot corresponds to a specific row index in the FLIM image (magenta line in Fig. 1B), which is linked to a corresponding CD68 stained immunohistological section (Fig. 1C).

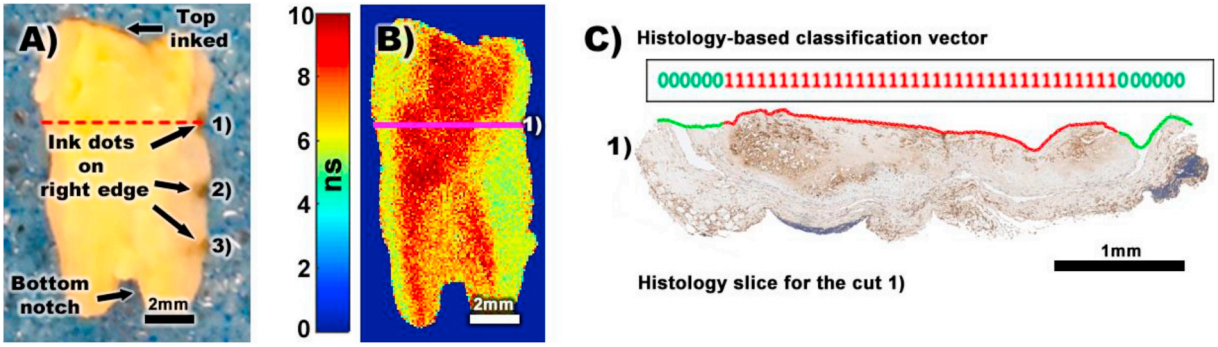

Fig. 1. Artery inking procedure and the correlation to the FLIM images.
(A) Photograph of a sample artery segment with the inked dots at the right side; the inked top edge and the bottom notch were used for orientation; the red dotted line indicates the approximate location of one of the tissue sections cut for histology. (B) Lifetime map (0–10 ns) of the 494 ± 20.5 nm channel with a magenta line indicating the correspondence of the row index with the first inked dot on the artery. (C) CD68 stained immunohistological section corresponding to the first inked dot and a graphic representation of the histology-based classification vector derived from lumen classification marks.

2.3. Immunohistological evaluation

CD68 staining was used to identify the presence of macrophages in the imaged coronary segments (Fig. 1C). Each CD68 stained histology section was visually evaluated (using Aperio ImageScope histology software from Leica Biosystems) for the presence of macrophages (MAC) by three researchers with expertise in histopathology and immunohistochemistry of coronary atherosclerosis (J.A.J., L.M.B., and D.V.), as follows: for each section, segments of the surface lumen were marked as either positive or negative for MAC presence (individual scattered cells were considered negative) within the intima area defined between the lumen and up to ~200 μm deep. The lengths of these segments were converted to proportions by dividing each segment length by the total length of the section's lumen. These proportions were used to generate a binary vector of size equal to the number of pixels in the corresponding row of the FLIM map, in order to label each FLIM pixel as either negative (0) or positive (1) for the presence of superficial MAC (gold standard labels).

2.4. Linear correlation analysis

Each histology section was divided in regions of interest (ROI) of ~500 μm long and ~200 μm deep (Fig. 2B). The percentage of CD68 staining of each ROI was visually estimated and used to quantify superficial MAC density. The mean values of the average fluorescence lifetime for each ROI was computed from the corresponding rows in the FLIM lifetime maps. Pearson linear correlation analysis was performed to test and quantify the linear correlation between the two variables. A *p*-value of less than 0.05 was chosen to indicate a significant linear correlation between CD68-based superficial MAC density and plaque lumen autofluorescence lifetime.

2.5. FLIM based detection of superficial macrophage infiltration

We have previously reported that the endogenous fluorescence emission from atherosclerotic plaques presenting lipids and macrophage accumulation show long lifetime values at wavelengths longer than ~450 nm [27]. Based on these observations, the proposed approach for detecting superficial macrophage infiltration is simply based on applying a threshold to the fluorescence lifetime values estimated from endogenous FLIM images acquired in the spectral channel of 494 ± 20.5 nm. The optimization of the fluorescence lifetime threshold was performed by applying the following Receiver Operating Characteristic (ROC) curve analysis. By applying a fluorescence lifetime threshold to each annotated FLIM map row (Fig. 1B), a corresponding FLIM-based classification vector was generated, where each pixel was assigned to either 1 (MAC positive: pixel-lifetime ≥ threshold-lifetime) or 0 (MAC negative: pixel-lifetime < threshold-lifetime). The classification performance estimated from matched CD68-based (gold standard) and FLIM-based binary classification vectors using different lifetime threshold values (from 0 to 12 ns, in steps of 0.08 ns) were then used to generate an ROC curve. An optimal fluorescence lifetime threshold value that would maximize classification accuracy while balancing sensitivity and specificity for detecting the presence of

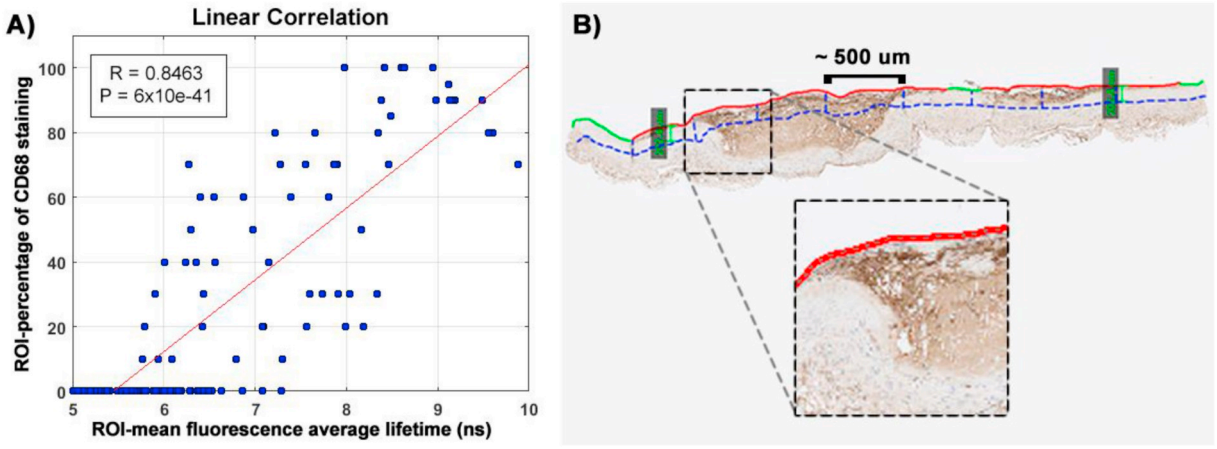

Fig. 2. Linear correlation plot (A) of the percentage of CD68 staining and the mean value of the average lifetimes of longitudinal ROI (~500 μm long and ~200 μm deep) of the artery sections (B).

superficial macrophages accumulation was selected from the generated ROC curve.

2.6. Cross validation

Two different cross-validation strategies were applied to estimate the classification performance of the proposed method. First, a 10-fold cross-validation method was performed as follows. The FLIM data from the 80 coronary segments were randomly split into 10 subsets, each from a random set of 8 coronary segments. At each of the 10 folds, an optimal lifetime threshold was identified by performing ROC analysis on nine of the 10 subsets, and the optimal lifetime threshold was applied to the data from the one testing subset not included on the ROC analysis. Values of overall classification accuracy, and sensitivity and specificity for detecting superficial MAC were then calculated from the pixel level classification of the testing subset data. After the 10 folds were performed, mean, standard deviation and median values were computed from the 10 estimations of overall classification accuracy, sensitivity, and specificity.

Second, a leave-one-subject-out cross-validation method was performed as follows. At each fold, an optimal lifetime threshold was identified by performing ROC analysis on the data from 22 out of the 23 subjects, and the optimal lifetime threshold was applied to the data from the one testing subject not included on the ROC analysis. Values of overall classification accuracy, and sensitivity and specificity for detecting superficial MAC were then calculated from the pixel level classification of the testing subject data. After the 23 folds were performed, mean, standard deviation and median values were computed from the 23 estimations of overall classification accuracy, sensitivity, and specificity.

3. Results

3.1. Linear correlation analysis

The correlation plot in Fig. 2A illustrates the strength of the linear correlation between ROI-percentage of CD68 staining in the histological images and the corresponding ROI-mean fluorescence average lifetime value from 24 randomly selected artery sections showing different degrees of superficial MAC density. Pearson linear correlation analysis on these two variables showed a statistically significant ($p < 10^{-41}$) and strong (R = 0.8463) linear correlation between MAC density (ROI-percentage of CD68 staining) and the fluorescence lifetime value (ROI-mean fluorescence average lifetime) at the 494 ± 20.5 nm emission band.

3.2. Threshold selection based on ROC analysis

The ROC curve (Fig. 3A) revealed an optimal fluorescence lifetime threshold of 6 ns, resulting in 91.56% accuracy, 87.92% sensitivity, and 91.83% specificity for detecting superficial MAC accumulation. The sample histograms in Fig. 3B shows two different distributions for the lifetime pixel values of the MAC and No-MAC groups identified using the CD68-based labeling (gold standard). Although the sample histograms of these groups show some overlap, they can clearly be separated by the selected fluorescence lifetime threshold of 6 ns (red dotted line in Fig. 3B).

3.3. Cross validation

The results of the two cross-validation strategies described in section 2.6 are shown in Table 1, which reports mean, standard deviation (S.D.) and median values of the estimates of overall classification accuracy, sensitivity and specificity for each fold. Overall, these estimates indicate values higher than 85% for the overall classification accuracy, sensitivity and specificity for detecting regions of atherosclerotic plaques with superficial macrophage accumulation.

3.4. Classification map

Once the optimal fluorescence lifetime threshold has been selected on the training dataset, the threshold can be applied to new fluorescence lifetime maps to generate binary classification maps highlighting the areas of the artery where superficial MAC accumulation has been identified. Fig. 4 shows examples of classification maps corresponding to three artery segments with varying degrees of MAC density. The first column (left) shows the fluorescence lifetime maps estimated from the endogenous FLIM images acquired in the spectral band of 494 ± 20.5 nm. The second column shows the color-coded binary classification maps, where pixels classified as having superficial MAC accumulation are shown in maroon, while pixels classified as not having superficial MAC accumulation are shown in green. The black (positive for MAC) and white (negative for MAC) lines superimposed on both the fluorescence lifetime and classification maps represent the CD68-based binary gold standard classification vector corresponding to each CD68 stained histology section (S1 to S9). The third column shows the CD68 stained histology sections (S1 to S9), where the red and green lines on the lumen indicate positive and negative for macrophage CD68 staining, respectively.

Sample 1 (Fig. 4A–C) corresponds to a coronary plaque segment showing extended areas with superficial MAC accumulation. The lifetime map (Fig. 4A) exhibits lifetime values in the range of 4–12 ns, and the superimposed CD68-based binary vector (black and white lines) show that areas with long fluorescence lifetime values correspond to positive CD68 staining (black segments). The binary classification map (Fig. 4B) indicates that the majority of the intimal surface shows detected superficial MAC accumulation, which is mostly in agreement with the histological sections (S2−S3) showing extended CD68 stained regions (Fig. 4C). However, the automated classification for S1 led to ~40% false positives (magenta arrow in Fig. 4B), which might be due to scattered MAC infiltration and/or imperfect spatial registration of the histology section on the FLIM map.

Sample 2 (Fig. 4D–F) corresponds to a coronary plaque segment showing focal areas with superficial MAC accumulation. The lifetime map (Fig. 4D) exhibits a large center area (and other much smaller ones) of long lifetime values, surrounded by areas with lifetime values around or below 5 ns. The superimposed CD68-based binary vector (black and white lines) show that the large center area with long fluorescence lifetime values corresponds to positive CD68 staining (black segments). The binary classification map (Fig. 4E) exhibits a large center area (and other much smaller ones) with detected superficial MAC accumulation, which is in agreement with the histological sections (S4−S7) showing CD68 stained regions in the center area of the coronary segment (Fig. 4F).

Sample 3 (Fig. 4G–I) corresponds to a coronary plaque segment without superficial MAC accumulation. The lifetime map (Fig. 4G) shows homogenous spatial distribution of lifetime values around or below 5 ns (except for two small focal areas with lifetime values ~6ns), corresponding to negative CD68 staining indicated by the superimposed CD68-based binary vector (white line). The binary classification map (Fig. 4H) indicates almost no presence of detected superficial MAC accumulation (except for two small false positive focal areas, magenta arrows), which is in agreement with the histological sections (S8−S9) showing no perceivable CD68 stained areas (Fig. 4I).

3.5. Intravascular FLIM based detection of superficial macrophage infiltration

To demonstrate intravascular detection of superficial macrophage accumulation, intravascular FLIM imaging of a fresh coronary segment was performed using an intravascular FLIM system with lateral resolution of < 100 μm and pull-back velocity > 10 mm/s [33]. The

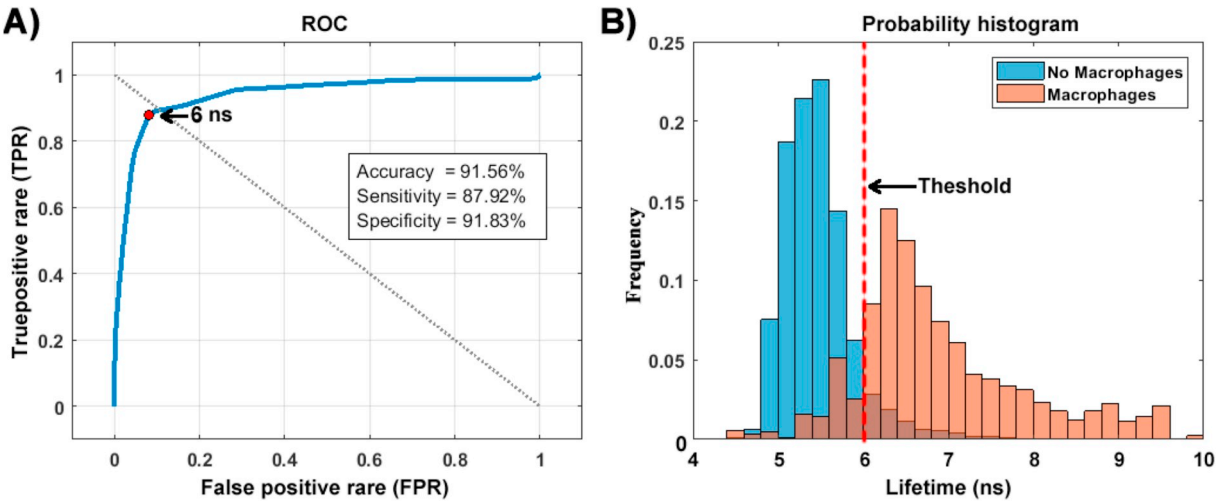

Fig. 3. (A) ROC curve showing the identified optimal threshold (6 ns, red dot). (B) Sample histograms of the average lifetime values of the MAC and No-MAC groups identified based on the CD68-based labeling. The red dashed line indicates the 6 ns threshold. (For interpretation of the references to color in this figure legend, the reader is referred to the Web version of this article.)

intravascular FLIM image of this coronary segment was acquired at a pull-back velocity of 10 mm/s using an excitation wavelength of 375 nm and an emission spectral band of 525 ± 25 nm. The imaged coronary segment was ink marked to allow the approximate determination of both the longitudinal position and orientation of the histological section produced with respect to the intravascular FLIM image. Changes in the distance between the catheter and the vessel wall were not controlled neither accounted for; therefore, there is almost certainly variation in pixel size as a function of radial position that was not corrected for. Nevertheless, it was possible to clearly identify areas with long autofluorescence lifetimes in the intravascular FLIM image (Fig. 5A) that correlated with plaques areas with significant superficial CD68 staining in the corresponding histological section (Fig. 5C), as indicated by the red arrows. The optimal threshold of 6 ns previously identified was applied to the intravascular FLIM image in order to generate a color-coded binary classification map, where areas classified as having superficial MAC accumulation are shown in maroon (Fig. 5B), which also correspond to areas with positive CD68 staining (Fig. 5C), as indicated by the red arrows.

4. Discussion

This study first demonstrated a strong linear correlation between the intimal autofluorescence lifetime measured at an emission band of 494 ± 20.5 nm and the degree of superficial macrophage accumulation (section 3.1; Fig. 2). These results suggest the feasibility for developing calibration curves that could enable quantifying the degree of superficial macrophage accumulation based on endogenous intravascular FLIM imaging. Since fluorescence lifetime measurements are insensitive to light intensity sensing artifacts, a potential technology for quantifying superficial macrophage infiltration based on FLIM would have significant advantage over other optical methods, including intravascular near infrared spectroscopy (NIRS) [34].

This study also demonstrated that an optimal threshold applied to the intimal autofluorescence lifetime measured at an emission band of 494 ± 20.5 nm enables the accurate detection of superficial macrophage accumulation within coronary atherosclerotic plaques (section 3.2-3.3; Fig. 3). By applying this threshold to endogenous FLIM images of coronary atherosclerotic plaques, intimal regions with significant superficial macrophage accumulation can be directly detected and visualized (section 3.4; Fig. 4).

In addition to its capability to accurately detect superficial macrophage accumulation, another significant advantage of this method is its simplicity. Since this method only requires measuring the autofluorescence lifetime of the intima at a single emission spectral band, the required intravascular FLIM instrumentation can be greatly simplified. As the detection of superficial macrophage accumulation requires just comparing the measured intimal autofluorescence lifetime to a threshold lifetime value, detection and visualization of intimal regions exhibiting significant superficial macrophage accumulation can be performed in real time. Based on our linear correlation results, we are also currently developing a calibration curve that would enable quantifying the degree of superficial macrophage accumulation based on endogenous intravascular FLIM imaging. This simple quantitative method could potentially enable real-time quantification and visualization of the degree of superficial macrophage accumulation.

The results of this study demonstrate that endogenous FLIM imaging can enable accurate assessment of plaque superficial macrophage infiltration, a key biomarker of plaque destabilization. Therefore, when used in conjunction with and/or integrated to other noninvasive and/or intravascular imaging modalities that can assess other key biomarker of plaque destabilization, endogenous FLIM imaging has the potential to play a key role in the clinical prediction of future coronary events.

The main limitation of this study is that the FLIM images used for quantifying the accuracy of our proposed method were acquired from cut opened fresh human coronary segments using a bench top FLIM imaging system. Although we have successfully applied this method to an intravascular FLIM image from a fresh human coronary segment

Table 1
Cross-validation analysis.

	10-fold (n = 10)			Leave-one-subject-out (n = 23)		
	Accuracy %	Sensitivity %	Specificity %	Accuracy %	Sensitivity %	Specificity %
Mean ± S.D.	88.71 ± 6.3	81.77 ± 23	88.9 ± 7.2	86.4 ± 11.7	82.29 ± 29.4	86.46 ± 13.4
Median	87.82	89.73	87.73	88.51	94.11	91.69

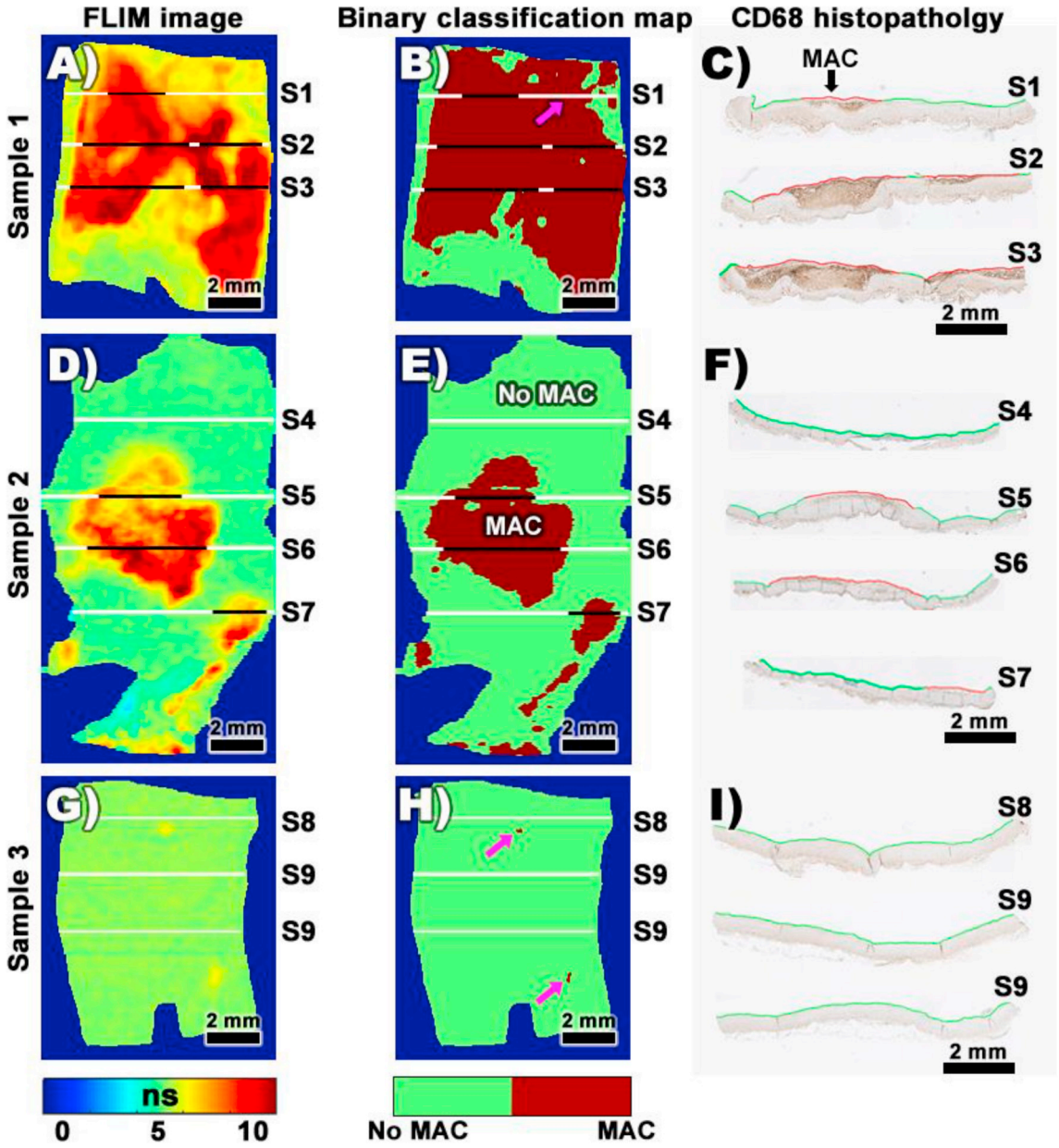

Fig. 4. Classification result of three sample artery segments with varying degrees of superficial MAC accumulation.
(A, D, G) Fluorescence lifetime maps estimated from the endogenous FLIM images acquired in the 494 ± 20.5 nm emission spectral band. (B, E, H) Color-coded binary classification maps, where pixels classified as having superficial MAC accumulation are shown in maroon, while pixels classified as not having superficial MAC accumulation are shown in green. The black and white lines on the lifetime and classification maps represent the CD68-based binary classification vector for each histology section (S1 to S9). (C, F, I) Photographs of each CD68 stained histological sections, where the red and green lines on the lumen indicate positive and negative for macrophage CD68 staining (gold standard).

(section 3.5; Fig. 5), a more extensive intravascular FLIM imaging validation is required. Another limitation is the limited interrogation depth (~200 μm) of endogenous FLIM plaque imaging; however, since macrophage infiltration within the thin cap of fibroatheromas is a particularly relevant biomarker of plaque vulnerability, this limitation can actually be advantageous. The presented preliminary results from intravascular FLIM data are already encouraging, as they suggest that the same fluorescence lifetime threshold identified using the benchtop FLIM data enabled detecting plaque areas with significant macrophage infiltration in spite of the mentioned differences in the FLIM imaging systems. These results also highlight the advantage of fluorescence lifetime measurements which are less sensitive to intensity artifacts, such as those potentially introduced by variations in the catheter/vessel-wall distance.

It is very likely that more than one endogenous fluorophore contributes to the plaque autofluorescence emission at the selected emission spectral band (494 ± 20.5 nm). However, regardless of which specific fluorophores contribute to the plaque autofluorescence emission at this specific emission spectral band, the results of this study clearly indicate that: i) plaque areas with superficial CD68 staining present long fluorescence lifetime values, and ii) the plaque autofluorescence lifetime enables the accurate detection of plaque areas with significant superficial CD68 staining. The scavenger receptor CD68 can be significantly upregulated in macrophages responding to inflammatory stimuli and is able to bind and internalize oxLDL [35]. Therefore, plaque areas with significant CD68 staining can indicate the presence of macrophages and/or oxLDL, which can be reliably assessed by endogenous FLIM imaging as demonstrated in this study. Our data

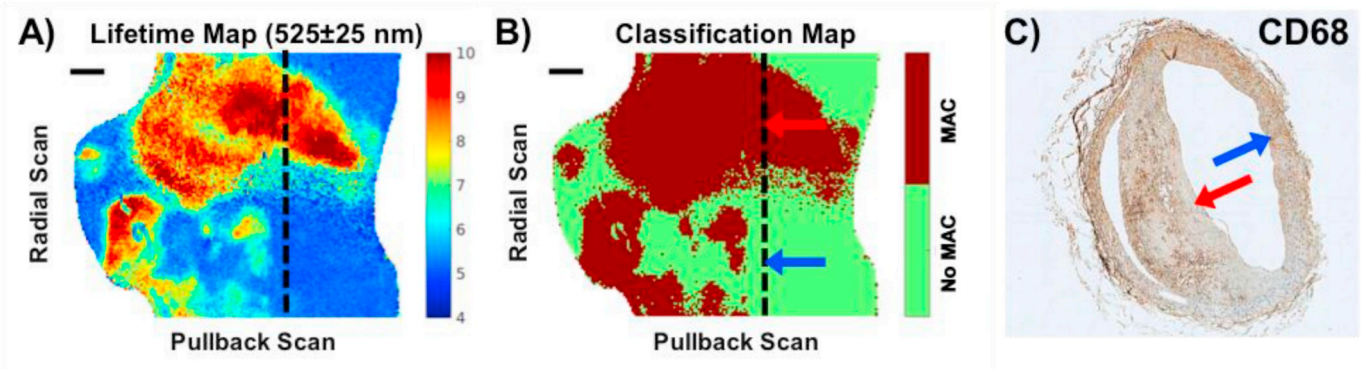

Fig. 5. Validation results on intravascular FLIM scan of fresh coronary segment.
(A) The autofluorescence lifetime map measured at an emission spectral band of 525 ± 25 nm shows different areas of long lifetime values (> 6 ns). (B) The optimal threshold of 6ns was applied to the autofluorescence lifetime map in order to generate a color-coded binary classification map (Maroon: superficial MAC accumulation; Green: no superficial MAC accumulation). (C) Histological section taken from the approximate location marked by dashed lines in (A) and (B) shows two regions: thick intima with significant CD68 staining corresponding to MAC positive area in the classification map (red arrow); thin intima with minimal CD68 staining corresponding to a MAC negative area in the classification map (blue arrow). Scale bar: 1 mm.

showed that the autofluorescence lifetime measured from the lumen of the plaques can identify plaque areas that show positive CD68 staining (sensitivity and specificity > 80%), which is an accepted (although not perfect) immunohistological staining for detecting macrophages in atherosclerotic plaques. Moreover, we observed that negative CD68 stained histological sections considered in our analysis corresponded to a variety of histopathological conditions including intimal thickening, fibrotic plaque, fibroatheroma with a thick fibrotic cap, and fibro-calcific plaque, which are all characterized by minimal macrophage infiltration.

Although the spatial resolution of the intravascular FLIM imaging system was limited (~100 μm), it is perfectly possible to design an intravascular FLIM imaging system with significantly better optical resolution (< 50 μm). As the optical resolution gets better, however, the number of pixels needed to image an equivalent area will increase, resulting in longer imaging time. Therefore, there is a tread-off between the optical resolution and the imaging speed of the intravascular FLIM imaging system. In order to attain practical imaging speeds for intravascular imaging (in the order of 10's mm/s pullback speed), we have kept the optical resolution at ~100 μm; nevertheless, we continue improving the specifications of our intravascular FLIM imaging systems. Alternatively, two-photon excitation (2 PE) FLIM would enable interrogating deeper into the coronary plaque with superior spatial and axial resolution; however, currently available laser, optical fiber and signal acquisition technologies are still not mature enough to enable the implementation of two-photon FLIM as a practical intravascular imaging modality.

A major disadvantage of our proposed approach is its invasiveness. Although noninvasive imaging modalities have the potential for imaging plaque macrophages, they still present several hurdles, particularly when focused on small and constantly moving coronary arteries, including the need of radiation exposure and exogenous contrast agents, limited spatial resolution, and susceptibility to motion artifacts [20]. Endogenous intravascular FLIM imaging, on the other hand, has the spatial resolution, sensitivity and specificity needed to enable the reliable detection of superficial macrophage accumulation in coronary plaques. Nevertheless, both noninvasive and intravascular imaging modalities could play different but complementary key roles in the preclinical and clinical imaging of macrophages in coronary atherosclerotic plaques, and potentially in the clinical management of CAD patients.

Macrophages play an important role in the development and destabilization of advanced atherosclerotic plaques [11]; hence, the clinical imaging of macrophage content in advanced plaques could potentially aid in identifying patients most at risk of future clinical events [12]. Several promising alternative therapeutic strategies targeting proatherogenic mechanisms in macrophages are currently being explored; therefore, the pre-clinical and clinical imaging of macrophage content in advanced plaques will also be essential for assessing efficacy of potential therapeutic strategies before committing to expensive and long-term end point trials [12]. Our novel and simple endogenous FLIM based method for detecting and potentially quantifying the presence and degree of superficial macrophage content in atherosclerotic plaques thus has great potential to become an intravascular imaging tool for assisting with both identifying patients most at risk of future clinical events and assessing efficacy of potential therapeutic strategies.

Conflicts of interest

The authors declared they do not have anything to disclose regarding conflict of interest with respect to this manuscript.

Author contributions

J.J. Rico-Jimenez: Designed the data analysis methodology; analyzed the data, wrote the manuscript. M.J. Serafino, S. Shrestha, X. Chen, W. Kim: Designed and built the FLIM instrumentation; imaged the coronary samples. J. Adame: Resected the coronary segments; prepared the coronary segments for imaging. M. Buja, D. Vera: Performed independent immunohistological evaluation. B.E. Applegate: Co-designed the research study; co-edited the manuscript. J.A. Jo: Co-designed and coordinated the research study; performed independent the immunohistological evaluation; co-edited the manuscript.

Acknowledgements

This project was supported by the National Institutes of Health (NIH grants 1R01HL111361 and 1R01CA218739). We would also like to acknowledge Dr. Brian L. Walton (University of Texas Health Science Center, Houston, Texas, USA) for providing inputs on the design of the study and the discussion of the results.

References

[1] S. Yusuf, S. Reddy, S. Ôunpuu, S. Anand, Global burden of cardiovascular diseases, Circulation 104 (2001) 2855–2864 http://circ.ahajournals.org/content/104/23/2855.abstract.
[2] R. Ross, Atherosclerosis is an inflammatory disease, Am. Heart J. 138 (1999) S419–S420, https://doi.org/10.1016/S0002-8703(99)70266-8.
[3] R. Stocker, J.F. Keaney, Role of oxidative modifications in atherosclerosis, Physiol. Rev. 84 (2004) 1381–1478, https://doi.org/10.1152/physrev.00047.2003.
[4] R. Virmani, A.P. Burke, A. Farb, F.D. Kolodgie, Pathology of the vulnerable plaque,

J. Am. Coll. Cardiol. 47 (2006) C13–C18 https://doi.org/10.1016/j.jacc.2005.10.065.
[5] J. Narula, M. Nakano, R. Virmani, F.D. Kolodgie, R. Petersen, R. Newcomb, S. Malik, V. Fuster, A. V Finn, Histopathologic characteristics of atherosclerotic coronary disease and implications of the findings for the invasive and noninvasive detection of vulnerable plaques, J. Am. Coll. Cardiol. 61 (2013) 1041–1051 https://doi.org/10.1016/j.jacc.2012.10.054.
[6] U. Garbin, E. Baggio, C. Stranieri, A. Pasini, S. Manfro, C. Mozzini, P. Vallerio, G. Lipari, F. Merigo, G. Guidi, L. Cominacini, A. Fratta Pasini, Expansion of necrotic core and shedding of Mertk receptor in human carotid plaques: a role for oxidized polyunsaturated fatty acids? Cardiovasc. Res. 97 (2013) 125–133 https://doi.org/10.1093/cvr/cvs301.
[7] H. Tao, P.G. Yancey, V.R. Babaev, J.L. Blakemore, Y. Zhang, L. Ding, S. Fazio, M.F. Linton, Macrophage SR-BI mediates efferocytosis via Src/PI3K/Rac1 signaling and reduces atherosclerotic lesion necrosis, J. Lipid Res. 56 (2015) 1449–1460 http://www.jlr.org/content/56/8/1449.abstract.
[8] E. Thorp, G. Li, T.A. Seimon, G. Kuriakose, D. Ron, I. Tabas, Reduced apoptosis and plaque necrosis in advanced atherosclerotic lesions of apoe-/- and Ldlr-/- mice Lacking CHOP, Cell Metabol. 9 (2009) 474–481, https://doi.org/10.1016/j.cmet.2009.03.003.
[9] T.A. Seimon, M.J. Nadolski, X. Liao, J. Magallon, M. Nguyen, N.T. Feric, M.L. Koschinsky, R. Harkewicz, J.L. Witztum, S. Tsimikas, D. Golenbock, K.J. Moore, I. Tabas, Atherogenic lipids and lipoproteins trigger CD36-TLR2-dependent apoptosis in macrophages undergoing endoplasmic reticulum stress, Cell Metabol. 12 (2010) 467–482, https://doi.org/10.1016/j.cmet.2010.09.010.
[10] P. Libby, Collagenases and cracks in the plaque, J. Clin. Investig. 123 (2013) 3201–3203, https://doi.org/10.1172/JCI67526.
[11] I. Tabas, K.E. Bornfeldt, Macrophage phenotype and function in different stages of atherosclerosis, Circ. Res. 118 (2016) 653 LP-667 http://circres.ahajournals.org/content/118/4/653.abstract.
[12] J.M. Tarkin, M.R. Dweck, N.R. Evans, R.A.P. Takx, A.J. Brown, A. Tawakol, Z.A. Fayad, J.H.F. Rudd, Imaging atherosclerosis, Circ. Res. 118 (2016) 750–769, https://doi.org/10.1161/CIRCRESAHA.115.306247.
[13] M. Drechsler, R. de Jong, J. Rossaint, J.R. Viola, G. Leoni, J.M. Wang, J. Grommes, R. Hinkel, C. Kupatt, C. Weber, Y. Döring, A. Zarbock, O. Soehnlein, Annexin A1 counteracts chemokine-induced arterial myeloid cell recruitment, Circ. Res. 116 (2015) 827 LP-835 http://circres.ahajournals.org/content/116/5/827.abstract.
[14] D.R. Lewis, L.K. Petersen, A.W. York, K.R. Zablocki, L.B. Joseph, V. Kholodovych, R.K. Prud'homme, K.E. Uhrich, P. V Moghe, Sugar-based amphiphilic nanoparticles arrest atherosclerosis in vivo, Proc. Natl. Acad. Sci. 112 (2015) 2693 LP-2698 http://www.pnas.org/content/112/9/2693.abstract.
[15] R. Duivenvoorden, J. Tang, D.P. Cormode, A.J. Mieszawska, D. Izquierdo-Garcia, C. Ozcan, M.J. Otten, N. Zaidi, M.E. Lobatto, S.M. van Rijs, B. Priem, E.L. Kuan, C. Martel, B. Hewing, H. Sager, M. Nahrendorf, G.J. Randolph, E.S.G. Stroes, V. Fuster, E.A. Fisher, Z.A. Fayad, W.J.M. Mulder, A statin-loaded reconstituted high-density lipoprotein nanoparticle inhibits atherosclerotic plaque inflammation, Nat. Commun. 5 (2014) 3065 https://doi.org/10.1038/ncomms4065.
[16] J. Bucerius, V. Mani, C. Moncrieff, J. Machac, V. Fuster, M.E. Farkouh, A. Tawakol, J.H.F. Rudd, Z.A. Fayad, Optimizing 18F-FDG PET/CT imaging of vessel wall inflammation: the impact of 18F-FDG circulation time, injected dose, uptake parameters, and fasting blood glucose levels, Eur. J. Nucl. Med. Mol. Imaging 41 (2014) 369–383, https://doi.org/10.1007/s00259-013-2569-6.
[17] J.M. Tarkin, F.R. Joshi, J.H.F. Rudd, PET imaging of inflammation in atherosclerosis, Nat. Rev. Cardiol. 11 (2014) 443–457 https://doi.org/10.1038/nrcardio.2014.80.
[18] E.J. Folco, Y. Sheikine, V.Z. Rocha, T. Christen, E. Shvartz, G.K. Sukhova, M.F. Di Carli, P. Libby, Hypoxia but not inflammation augments glucose uptake in human macrophages: implications for imaging atherosclerosis with 18fluorine-labeled 2-deoxy-D-glucose positron emission tomography, J. Am. Coll. Cardiol. 58 (2011) 603–614 https://doi.org/10.1016/j.jacc.2011.03.044.
[19] J. Wykrzykowska, S. Lehman, G. Williams, J.A. Parker, M.R. Palmer, S. Varkey, G. Kolodny, R. Laham, Imaging of inflamed and vulnerable plaque in coronary arteries with 18F-FDG PET/CT in patients with suppression of myocardial uptake using a low-carbohydrate, high-fat preparation, J. Nucl. Med. 50 (2009) 563–568 http://jnm.snmjournals.org/content/50/4/563.abstract.
[20] M.E. Kooi, V.C. Cappendijk, K.B.J.M. Cleutjens, A.G.H. Kessels, P.J.E.H.M. Kitslaar, M. Borgers, P.M. Frederik, M.J.A.P. Daemen, J.M.A. van Engelshoven, Accumulation of ultrasmall superparamagnetic particles of iron oxide in human atherosclerotic plaques can Be detected by in vivo magnetic resonance imaging, Circulation 107 (2003) 2453–2458, https://doi.org/10.1161/01.CIR.0000068315.98705.CC.
[21] K. Morishige, D.F. Kacher, P. Libby, L. Josephson, P. Ganz, R. Weissleder, M. Aikawa, High-resolution magnetic resonance imaging enhanced with superparamagnetic nanoparticles measures macrophage burden in atherosclerosis, Circulation 122 (2010) 1707 LP-1715 http://circ.ahajournals.org/content/122/17/1707.abstract.
[22] M.R. Makowski, M. Henningsson, E. Spuentrup, W.Y. Kim, D. Maintz, W.J. Manning, R.M. Botnar, Characterization of coronary atherosclerosis by magnetic resonance imaging, Circulation 128 (2013) 1244 LP-1255 http://circ.ahajournals.org/content/128/11/1244.abstract.
[23] R.A. Trivedi, C. Mallawarachi, J.-M. U-King-Im, M.J. Graves, J. Horsley, M.J. Goddard, A. Brown, L. Wang, P.J. Kirkpatrick, J. Brown, J.H. Gillard, Identifying inflamed carotid plaques using in vivo USPIO-enhanced MR imaging to label plaque macrophages, Arterioscler. Thromb. Vasc. Biol. 26 (2006) 1601 LP-1606 http://atvb.ahajournals.org/content/26/7/1601.abstract.
[24] S.P.S. Howarth, T.Y. Tang, R. Trivedi, R. Weerakkody, J. U-King-Im, M.E. Gaunt, J.R. Boyle, Z.Y. Li, S.R. Miller, M.J. Graves, J.H. Gillard, Utility of USPIO-enhanced MR imaging to identify inflammation and the fibrous cap: a comparison of symptomatic and asymptomatic individuals, Eur. J. Radiol. 70 (2009) 555–560 https://doi.org/10.1016/j.ejrad.2008.01.047.
[25] G.J. Tearney, H. Yabushita, S.L. Houser, H.T. Aretz, I.-K. Jang, K.H. Schlendorf, C.R. Kauffman, M. Shishkov, E.F. Halpern, B.E. Bouma, Quantification of macrophage content in atherosclerotic plaques by optical coherence tomography, Circulation 107 (2003) 113–119 http://circ.ahajournals.org/content/107/1/113.abstract.
[26] J.E. Phipps, D. Vela, T. Hoyt, D.L. Halaney, J.J. Mancuso, L.M. Buja, R. Asmis, T.E. Milner, M.D. Feldman, Macrophages and intravascular OCT bright spots: a quantitative study, JACC Cardiovasc. Imaging 8 (2015) 63–72 https://doi.org/10.1016/j.jcmg.2014.07.027.
[27] S. Lee, M.W. Lee, H.S. Cho, J.W. Song, H.S. Nam, D.J. Oh, K. Park, W.-Y. Oh, H. Yoo, J.W. Kim, Fully integrated high-speed intravascular optical coherence tomography/near-infrared fluorescence structural/molecular imaging in vivo using a clinically available near-infrared fluorescence–emitting indocyanine green to detect inflamed lipid-rich atherom, Circ. Cardiovasc. Interv. 7 (2014) 560–569 http://circinterventions.ahajournals.org/content/7/4/560.abstract.
[28] J.A. Jo, J. Park, P. Pande, S. Shrestha, M.J. Serafino, J. de J. Rico Jimenez, F. Clubb, B. Walton, L.M. Buja, J.E. Phipps, M.D. Feldman, J. Adame, B.E. Applegate, Simultaneous morphological and biochemical endogenous optical imaging of atherosclerosis, Eur. Hear. J. - Cardiovasc. Imaging. 16 (2015) 910–918, https://doi.org/10.1093/ehjci/jev018.
[29] J. Bec, J.E. Phipps, D. Gorpas, D. Ma, H. Fatakdawala, K.B. Margulies, J.A. Southard, L. Marcu, In vivo label-free structural and biochemical imaging of coronary arteries using an integrated ultrasound and multispectral fluorescence lifetime catheter system, Sci. Rep. 7 (2017) 8960, https://doi.org/10.1038/s41598-017-08056-0.
[30] S. Shrestha, M.J. Serafino, J. Rico-Jimenez, J. Park, X. Chen, S. Zhaorigetu, B.L. Walton, J.A. Jo, B.E. Applegate, Multimodal optical coherence tomography and fluorescence lifetime imaging with interleaved excitation sources for simultaneous endogenous and exogenous fluorescence, Biomed. Opt. Express 7 (2016) 3184–3197, https://doi.org/10.1364/BOE.7.003184.
[31] A. Grinvald, I.Z. Steinberg, On the analysis of fluorescence decay kinetics by the method of least-squares, Anal. Biochem. 59 (1974) 583–598 https://doi.org/10.1016/0003-2697(74)90312-1.
[32] J. Park, J.A. Jo, S. Shrestha, P. Pande, Q. Wan, B.E. Applegate, A dual-modality optical coherence tomography and fluorescence lifetime imaging microscopy system for simultaneous morphological and biochemical tissue characterization, Biomed. Opt. Express 1 (2010) 186–200, https://doi.org/10.1364/BOE.1.000186.
[33] X. Chen, W. Kim, M.J. Serafino, Z. Tan, B. Walton, L.M. Buja, J. Adame, J.A. Jo, B.E. Applegate, Design and Validation of the Ball Lens-Based Intravascular Catheter for Fluorescence Lifetime Imaging Microscopy of Atherosclerosis (Conference Presentation), 2018, p. 1047102 https://doi.org/10.1117/12.2287447.
[34] J.-C. Tardif, M.-J. Bertrand, K. Kyprianidis (Eds.), Near-Infrared Spectroscopy (NIRS): A Novel Tool for Intravascular Coronary Imaging, InTech, Rijeka, 2017, , https://doi.org/10.5772/67196 Ch. 2.
[35] D.A. Chistiakov, M.C. Killingsworth, V.A. Myasoedova, A.N. Orekhov, Y. V Bobryshev, CD68/macrosialin: not just a histochemical marker, Lab. Invest. 97 (2017) 4–13, https://doi.org/10.1038/labinvest.2016.116.